Influence of asymmetry and nodal structures on high-harmonic generation in heteronuclear molecules

B B Augstein, C Figueira De, Morisson Faria

Influence of asymmetry and nodal structures on high-harmonic generation in heteronuclear molecules

B. B. Augstein and C. Figueira de Morisson Faria

Department of Physics and Astronomy, University College London, Gower Street, London WC1E 6BT, United Kingdom

Abstract. The relation between high-harmonic spectra and the geometry of the molecular orbital in position and momentum space is investigated. In particular we choose two isoelectronic pairs of homonuclear and heteronuclear molecules, such that the highest occupied molecular orbital of the former exhibits at least one nodal plane. The imprint of such planes is a strong suppression in the harmonic spectra, for particular alignment angles. We are able to identify two distinct types of nodal structures. If, for homonuclear molecules, the nodal planes are determined by the atomic wavefunctions only, the angle for which the yield is suppressed will remain the same for both types of molecules. In contrast, if they are determined by the linear combination of atomic orbitals at different centers of the molecule, there will be a shift in the angle at which the suppression occurs and a distortion in the nodal structure for the heteronuclear molecule, with respect to its homonuclear counterpart. This shows that, in principle, molecular imaging, in which homonuclear molecule is used as a reference while observing the wavefunction distortions in its heteronuclear counterpart, is possible.

PACS numbers: 33.80.Rv, 42.65.Ky

1. Introduction

High harmonic generation, first discovered in the late 1980s [1], is a process which occurs when atoms or molecules are exposed to intense laser fields, and results in the emission of high frequency coherent radiation. It can be readily understood in terms of the three step model, [2, 3], where an electron is ionized from the atom or molecule, propagates in the laser field, and recombines with its parent ion, upon which high harmonics are released.

Currently, there is much interest in this process due to the possibility of tomographic orbital reconstruction [4, 5, 6], and the study of quantum interference effects [7, 8, 9]. In particular quantum-interference minima and maxima due to high-harmonic emission at spatially separated centers, and high-harmonic suppression due to the presence of nodal planes in the orbital wavefunctions, have been identified and discussed theoretically. Such studies have been extensively performed in diatomic molecules [6, 7, 8, 9, 10, 15, 20]. In many of these studies so far, homonuclear molecules with definite orbital symmetry, either gerade or ungerade, have mostly been used, whereas heteronuclear molecules driven by strong fields are now starting to attract attention [11, 12, 13]. The orbital wavefunctions in such molecules do not have a definite orbital symmetry. Furthermore, heteronuclear molecules also contain a static dipole moment. These attributes will affect the harmonic spectra and the observables related to other strong field phenomena. Hence, a legitimate question to ask is whether two-center interference patterns, or the imprint of nodal surfaces in general, in form of high-harmonic suppression, can still be observed in the spectra. This is specially interesting, since, experimentally, in the past few years, it has become possible to orient the permanent dipole moments of heteronuclear molecules with regard to the polarization direction of the driving field [11].

In this work, we compare isoelectronic homonuclear and heteronuclear molecules, with particular emphasis on nodal planes in the position space wavefunction and two-center interference effects. We assume the Born-Oppenheimer approximation to be valid, which should hold for large enough molecules [9]. Specifically, we take the pairs Be_2 and LiB, and O_2 and NF. The homonuclear molecule in the former and the latter pair have a σ_u and π_g highest occupied molecular orbital (HOMO), respectively. Such orbitals contain nodal planes which are altered when a heteronuclear counterpart is chosen. In our investigations, we employ the single-active electron and the strong-field approximation and assume that the HOMO is the only active orbital. The influence of multiple orbitals has been discussed elsewhere [6, 15, 16].

This work is organized as follows. In Sec. 2 the molecular orbital construction is briefly stated, and the three step model (Sec. 2.1), saddle-point equations (Sec. 2.2) and interference conditions (Sec. 2.3) are discussed. In Sec. 3, we present our results. This section is split into two main parts. First, in Sec. 3.1, we address the molecular orbitals obtained by us, with a particular emphasis on their nodal structures, or the absence thereof. Subsequently, in Sec. 3.2, we discuss how such characteristics manifest themselves in the spectra. Finally, in Sec. 4, we state the main conclusions to be drawn from this work. Unless otherwise stated, we use atomic units throughout.

2. Model

Below, we will discuss the transition amplitudes employed in this work, for homonuclear and heteronuclear molecules. The molecular orbitals are calculated using

the Linear Combination of Atomic Orbitals (LCAO) approximation, along with the Born Oppenheimer approximation. Under these assumptions, the molecular orbital wavefunction is given by

$$\Psi(\mathbf{r}) = \sum_{\alpha} c_{\alpha}^{(L)} \Phi_{\alpha}^{(L)}(\mathbf{r}+\mathbf{R}/2) + (-1)^{l_\alpha - m_\alpha + \lambda_\alpha} c_{\alpha}^{(R)} \Phi_{\alpha}^{(R)}(\mathbf{r}-\mathbf{R}/2) \quad (1)$$

where $\mathbf{R}$ is the internuclear separation, l_α is the orbital quantum number and m_α is the magnetic quantum number. We assume that the ions are positioned along the z axis, i.e., that $\mathbf{R} = R\hat{e}_z$. The coefficients $c_{\alpha}^{(\xi)}$ form the linear combination of atomic orbitals and are extracted from the quantum chemistry code GAMESS-UK [14]. The indices (L) and (R) refer to the left or to the right ion, respectively, which is a distinction required for heteronuclear molecules, whereas for homonuclear molecules, $c_{\alpha}^{(L)} = c_{\alpha}^{(R)} = c_\alpha$ and $\Phi_{\alpha}^{(R)} = \Phi_{\alpha}^{(L)} = \Phi_\alpha$. The internuclear axis is taken to be along the z direction in the molecular fixed frame, and the direction of the laser polarization defines the z axis in the lab frame. The parameter λ_α determines the orbital symmetry of the molecular orbital, with λ_α=$|m_\alpha|$ and λ_α=$|m_\alpha|$+1 for homonuclear molecules of gerade and ungerade symmetry, respectively. Throughout, we have employed Gaussian type orbitals with a real 6-31 basis set composed of only s and p states. We find that polarized basis sets make little difference to the orbital wavefunctions. For more details on these wavefunctions we refer to our previous work [15].

2.1. Transition amplitude

The transition amplitude for high harmonic generation, within the framework of of the strong field approximation (SFA) [2], reads as,

$$b_\Omega = -i \int_{-\infty}^{\infty} dt \int_{-\infty}^{t} dt' \int d^3k\, a_{\rm rec}^{*}(\mathbf{k}+\mathbf{A}(t)) a_{\rm ion}(\mathbf{k}+\mathbf{A}(t')) \exp[iS(t,t',\Omega,\mathbf{k})] + c.c., \quad (2)$$

with the action

$$S(t,t',\Omega,\mathbf{k}) = -\frac{1}{2}\int_{t'}^{t} [\mathbf{k}+\mathbf{A}(\tau)]^2 d\tau - E_0(t-t') + \Omega t \quad (3)$$

where $a_{\rm rec}(\mathbf{k}+\mathbf{A}(t)) = \langle \mathbf{k}+\mathbf{A}(t)|\, \mathbf{d}\cdot\mathbf{e}_x\, |\Psi\rangle$ and $a_{\rm ion}(\mathbf{k}+\mathbf{A}(t')) = \langle \mathbf{k}+\mathbf{A}(t')|\, \mathbf{E}(t')\cdot r\mathbf{e}_x\, |\Psi\rangle$, are the recombination and ionization dipole matrix elements, respectively. The terms $\mathbf{d}$, $\mathbf{e}_x$ and Ω denote the dipole operator and the laser-polarization vector and the harmonic frequency, respectively. The ionization potential of the highest occupied molecular orbital, denoted by $|\Psi\rangle$, is given by E_0. The length gauge is used throughout as the interference minima in the harmonic spectra vanish in the velocity gauge [17, 18], and the length form of the dipole operator is used as it accounts for the presence of the static dipole moment‡. In the present work, we are neglecting the time-dependent Stark shifts in the ionization potential. Recently, a modified SFA including

‡ In the length form, the dipole operator reads $\mathbf{d} = \mathbf{r}$. Recently, we have shown that if a Gaussian basis set is employed in the modeling of the molecular orbitals, the velocity form of the dipole operator leads to a vanishing static dipole moment in heteronuclear molecule. This problem is absent if the length form is taken. For details see [20].

such shifts has been developed and applied to heteronuclear molecules [12, 13]. As a first approximation, as long as the static dipole moments are small, such Stark shifts can be neglected.

Within the present framework, one may either incorporate the structure of the molecule in the dipole matrix elements, or in the action. If the former procedure is followed, all structural information about the molecular orbital is contained in the recombination matrix element, $a_{\rm rec}(\mathbf{k}+\mathbf{A}(t))$, which is given by

$$a_{\rm rec}(\mathbf{k}) = \frac{1}{(2\pi)^{3/2}} \int d^3r \mathbf{r}\cdot\hat{e}_z \exp[-i\mathbf{k}\cdot\mathbf{r}]\Psi(\mathbf{r}), \tag{4}$$

where $\Psi(\mathbf{r})$ is defined in Eq. (1). This is the component of $i\partial_{\mathbf{k}}\Psi(\mathbf{k})$ along the laser-field polarization, where

$$\begin{aligned}\psi(\mathbf{k}) = &\sum_\alpha \exp[i\mathbf{k}\cdot\frac{\mathbf{R}}{2}]c_\alpha^{(L)}\Phi_\alpha^{(L)}(\mathbf{k}) \\ &+ (-1)^{l_\alpha-m_\alpha+\lambda_\alpha}\exp[-i\mathbf{k}\cdot\frac{\mathbf{R}}{2}]c_\alpha^{(R)}\Phi_\alpha^{(R)}(\mathbf{k}),\end{aligned} \tag{5}$$

denotes the momentum-space wavefunction. This matrix element gives rise to any two center interference which occurs in the harmonic spectra. The ionization matrix element, $a_{\rm ion}(\mathbf{k}+\mathbf{A}(t'))$, on the other hand, will mainly determine whether tunnel ionization will be suppressed or enhanced due to the shape of a particular orbital. Therefore it directly affects the overall harmonic yield, but is not responsible for any interference patterns. Both matrix elements are vanishing for nodes in the molecular orbitals.

If the latter procedure is followed, this will lead to the coherent sum

$$M = \sum_{\mu,\nu} M_{\mu\nu} \tag{6}$$

over four distinct possible processes, where

$$\begin{aligned}M_{\mu\nu} = &-i\int_{-\infty}^{\infty}dt\int_{-\infty}^{t}dt'\int d^3k \mathcal{J}_{\mu\nu}(\mathbf{k},t,t') \\ &\exp[iS_{\mu\nu}(t,t',\Omega,\mathbf{k})] + c.c..\end{aligned} \tag{7}$$

The indices μ,ν refer to the left or right ion in the molecule, as L or R. Each of these terms will exhibit a similar form to Eq. (2), with $S(t,t',\Omega,\mathbf{k})$ replaced by the modified actions $S_{\mu\nu}(t,t',\Omega,\mathbf{k})$, where μ and ν indicate the ion with which the electron recombines and from which it is released, respectively. The prefactor $a^*_{\rm rec}(\mathbf{k}+\mathbf{A}(t))a_{\rm ion}(\mathbf{k}+\mathbf{A}(t'))$ will be replaced by

$$\mathcal{J}_{\mu\nu}(\mathbf{k},t,t') = \sum_{\alpha,\beta}\Xi_{\mu,\nu}c_\alpha^{*(\mu)}c_\beta^{(\nu)}\partial_{\mathbf{k}(t)}\Phi_\alpha^{*(\mu)}(\mathbf{k}(t))\partial_{\mathbf{k}(t')}\Phi_\beta^{(\nu)}(\mathbf{k}(t')), \tag{8}$$

where $\mathbf{k}(\tau) = \mathbf{k}+\mathbf{A}(\tau)$, with $\tau = t,t'$, and, once more, the indices μ,ν refer to the left or right ion. The coefficients $\Xi_{\mu,\nu}$ are introduced to account for the parity of the atomic wave functions composing the orbitals, such that $\Xi_{_{L,L}} = 1, \Xi_{_{R,L}} = (-1)^{l_\alpha-m_\alpha+\lambda_\alpha}, \Xi_{_{L,R}} = (-1)^{l_\beta-m_\beta+\lambda_\beta}$ and $\Xi_{_{R,R}} = \Xi_{_{L,R}}\Xi_{_{R,L}}$. The modified actions are defined as

$$S_{\nu\nu}(t,t',\Omega,\mathbf{k}) = S(t,t',\Omega,\mathbf{k}) \pm [\mathbf{A}(t)-\mathbf{A}(t')]\cdot\mathbf{R}/2 \tag{9}$$

for $\mu = \nu$, where the negative and positive signs apply to the left and right ion, respectively, and

$$S_{\mu\nu}(t, t', \Omega, \mathbf{k}) = S(t, t', \Omega, \mathbf{k}) \pm \mathbf{k} \cdot \mathbf{R} \pm [\mathbf{A}(t) + \mathbf{A}(t')] \cdot \mathbf{R}/2 \tag{10}$$

for $\mu \neq \nu$. In Eq. (10), the positive and negative signs correspond to S_{RL} and S_{LR}, respectively. We will show below that the action (9) leads to the so-called "direct harmonics", for which the active electron leaves and recombines with the same ion, while Eq. (10) gives the so-called "exchange harmonics", for which the electron tunnels from one ion and recombines with the other. Within the strong-field approximation, such harmonics have been first identified in [22]. For systematic studies of the exchange harmonics using saddle-point methods and a linear combination of $1s$ orbitals see [23, 18].

2.2. Saddle-point equations

To solve the HHG transition amplitude (2) we use the saddle-point approximation [19], i.e., we seek values for t, t' and $\mathbf{k}$ such that the action is stationary. This results in saddle-point equations which can be related to the orbits of an electron in an external laser field.

If one considers the transition amplitude (2), i.e., if one incorporates the influence of the molecule in the prefactor, then the saddle-point equations $\partial S(t, t', \Omega, \mathbf{k})/\partial t' = \partial S(t, t', \Omega, \mathbf{k})/\partial t = 0$ and $\partial S(t, t', \Omega, \mathbf{k})/\partial \mathbf{k} = \mathbf{0}$ lead to

$$\frac{[\mathbf{k} + \mathbf{A}(t')]^2}{2} + E_0 = 0, \tag{11}$$

$$\int_{t'}^{t} d\tau \, [\mathbf{k} + \mathbf{A}(\tau)] = \mathbf{0}. \tag{12}$$

and

$$\frac{[\mathbf{k} + \mathbf{A}(t)]^2}{2} + E_0 = \Omega. \tag{13}$$

These equations have the following physical interpretation. Initially the electron is tunnel ionized from the binding potential. This results in Eq. (11), which gives the conservation of energy. Note that this equation has only complex solutions, as a consequence of the fact that tunneling has no classical counterpart. Secondly, Eq. (12) results in the electron momentum in the continuum being constrained such that the electron returns to its place of origin, which we take to be the geometric center of the molecule. Finally, Eq. (13) represents conservation of energy at recombination. The return condition (12) guarantees that the momentum $\mathbf{k}$ and the external field are collinear. Hence, for a linearly polarized field the angle between the intermediate momentum $\mathbf{k}$ and the internuclear axis $\mathbf{R}$ is equal to the orientation angle θ_L between the molecule and the field.

If, on the other hand, one incorporates the molecular structure in the action, it will be necessary to distinguish between the direct and exchange harmonics. The former will lead to the saddle-point equations $\partial S_{\nu\nu}(t, t', \Omega, \mathbf{k})/\partial t' = \partial S_{\nu\nu}(t, t', \Omega, \mathbf{k})/\partial t = 0$ and $\partial S_{\nu\nu}(t, t', \Omega, \mathbf{k})/\partial \mathbf{k} = \mathbf{0}$, where $S_{\nu\nu}(t, t', \Omega, \mathbf{k})$ is given by Eq. (9). The latter can be obtained from the derivatives of $S_{\nu\mu}(t, t', \Omega, \mathbf{k}), \mu \neq \nu$, i.e., Eq. (10), with regard to t, t' and $\mathbf{k}$.

Tunnel ionization and recombination for both the direct and the exchange harmonics will be given by the saddle-point equations

$$\frac{[\mathbf{k}+\mathbf{A}(t')]^2}{2} + E_0 \pm \mathbf{E}(t')\cdot\mathbf{R}/2 = 0 \tag{14}$$

and

$$\frac{[\mathbf{k}+\mathbf{A}(t)]^2}{2} + E_0 \pm \mathbf{E}(t)\cdot\mathbf{R}/2 = \Omega. \tag{15}$$

The terms proportional to the field $\mathbf{E}(\tau), \tau = t, t'$, and to the internuclear distance $\mathbf{R}$ can be interpreted as potential-energy shifts, which appear due to the fact that the ions the molecule are displaced with regard to the origin of the coordinate system. These potential-energy shifts appear when the length-gauge formulation of the SFA is considered, and have raised a great deal of debate (for details see [23, 18]). For the direct harmonics generated at the left and the right ions ($\nu = L$ and $\nu = R$), one must take the negative and positive signs for the potential-energy shifts in Eqs. (14) and (15), respectively. In contrast, for the exchange harmonics, the potential-energy shifts in such equations exhibit opposite signs. Specifically, ionization from the left ion and recombination with the right ion will lead to negative sign in Eq. (14) and positive sign in Eq. (15), while these signs will be reversed if the electron is freed from the right ion and recombines with the left ion.

The return condition will remain the same as in the modified-prefactor case, with the difference that now the electron is returning to each ion, instead of to the geometric center of the molecule. For the exchange harmonics, the return condition will read

$$-\int_{t'}^{t} d\tau\,[\mathbf{k}+\mathbf{A}(\tau)] \pm \mathbf{R} = \mathbf{0}, \tag{16}$$

where the positive and negative signs correspond to $S_{RL}(t,t',\Omega,\mathbf{k})$ and $S_{LR}(t,t',\Omega,\mathbf{k})$, respectively. In the former case, the electron is released in the continuum from the left ion and recombines with the right ion, while in the latter case, ionization from the right ion and recombination with the left ion takes place. Eq. (6) also shows that the intermediate electron momentum is no longer collinear with regard to the external laser field. This has been pointed out recently in [24] as leading to elliptically polarized harmonics in molecules, from a linearly polarized driving field.

In the particular studies performed in this work, we are not considering the periodic contributions to high-order harmonic generation over many cycles. These would lead to sharp harmonic peaks, which would make the suppressions studied in this work more difficult to single out.

2.3. Interference Condition

Maxima and minima in the momentum-space wavefunction may be determined by writing the exponents in Eq. (5) in terms of trigonometric functions. In this case, one obtains

$$\psi(\mathbf{k}) = \sum_{\alpha} \mathcal{C}_{+}^{(\alpha)} \cos\left[\frac{\mathbf{k}\cdot\mathbf{R}}{2}\right] + i\mathcal{C}_{-}^{(\alpha)} \sin\left[\frac{\mathbf{k}\cdot\mathbf{R}}{2}\right], \tag{17}$$

with

$$\mathcal{C}_{\pm}^{(\alpha)} = (-1)^{l_\alpha - m_\alpha + \lambda_\alpha} c_\alpha^{(R)} \Phi_\alpha^{(R)}(\mathbf{k}) \pm c_\alpha^{(L)} \Phi_\alpha^{(L)}(\mathbf{k}). \tag{18}$$

Calling $\vartheta = \arctan[i\mathcal{C}_+^{(\alpha)}/\mathcal{C}_-^{(\alpha)}]$,we find

$$\psi(\mathbf{k}) = \sum_\alpha \sqrt{\left(\mathcal{C}_+^{(\alpha)}\right)^2 - \left(\mathcal{C}_-^{(\alpha)}\right)^2}\,\sin[\vartheta + \mathbf{k}\cdot\mathbf{R}/2]. \tag{19}$$

Eq. (19) exhibits minima for $\vartheta + \mathbf{k}\cdot\mathbf{R}/2 = n\pi$.

Note, however, that the coefficients $\mathcal{C}_\pm^{(\alpha)}$ defined in Eq. (18) depend on the wavefunctions at the left and right ions. Since these wavefunctions themselves depend on the momentum $\mathbf{k}$, one expects the two-center patterns to be blurred for heteronuclear molecules. In contrast, for homonuclear molecules, $c_\alpha^{(L)} = c_\alpha^{(R)}$ and $\Phi_\alpha^{(L)}(\mathbf{k}) = \Phi_\alpha^{(R)}(\mathbf{k})$. This implies that the momentum dependence in the argument ϑ cancels out and that the interference condition in Refs. [8, 15] is recovered. In this case, sharp interference fringes are expected to be present.

The above-stated condition does not only lead to interference fringes in the bound-state momentum wavefunctions but also in the high-harmonic spectra. This is due to the fact that the dipole matrix elements depend on the wavefunctions (5). In this latter case, $\mathbf{k} \to \mathbf{k} + \mathbf{A}(t)$ in Eqs. (5)-(19).

For a linearly polarized monochromatic field of frequency ω, using the saddle-point equation (15), the generalized interference condition (19) may be expressed in terms of the harmonic order n as

$$n = \frac{E_0}{\omega} + \frac{2(\kappa\pi - \vartheta)^2}{\omega R^2 \cos^2\theta_L}, \tag{20}$$

where E_0 is the absolute value of the bound-state energy in question, κ is an integer number, θ_L is the orientation angle, R is the internuclear distance and ϑ is defined above. This interference condition has been first derived in [21] and has been used by us in previous work [15].

In the specific case of orbitals of π_g type, which are constructed entirely from p-type atomic orbitals such that $l_\alpha = 1$, are of gerade symmetry such that $\lambda_\alpha = 0$, and are made from a homonuclear species such that $\Phi_\alpha^{(R)}(\mathbf{k}) = \Phi_\alpha^{(L)}(\mathbf{k})$ and $c_\alpha^{(R)} = c_\alpha^{(L)}$, one finds that $\vartheta = 0$. This implies that for the zeroth order interference, where $\kappa = 0$, the second term of (20) will vanish leaving the angular independent term

$$n = \frac{E_0}{\omega}. \tag{21}$$

This minimum, however, would occur exactly at the ionization threshold, for which the present framework is expected to break down. Hence, it will not be discussed here.

3. Results

3.1. Position and momentum space wavefunctions

In this section, we will display the specific molecular orbitals employed by us when calculating the results that follow. We choose two pairs of molecules composed of a homonuclear molecule and an isoelectronic heteronuclear molecule. The first pair, Be_2 and LiB, possess eight electrons and a σ highest occupied molecular orbital, while the second pair, O_2 and NF, have sixteen electrons and a π highest occupied molecular orbital.

In Fig. 1, we exhibit the HOMO for homonuclear molecules, Be_2 and O_2, and heteronuclear molecules, LiB and NF, as obtained with GAMESS-UK [Figs. 1.(a),(c),(b) and (d) respectively]. The internuclear axis is chosen to be along

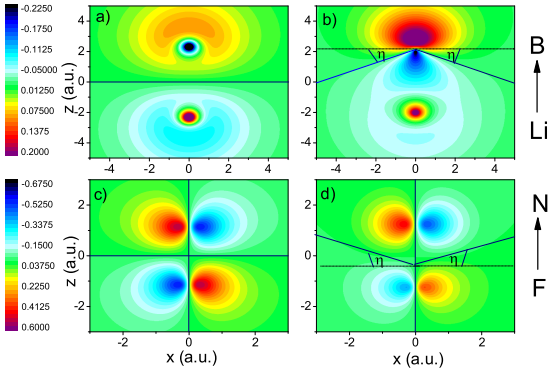

Figure 1. Highest occupied molecular orbitals in position space for the homonuclear molecules Be_2 and O_2 [panels a) and c)], and their heteronuclear isoelectronic counterparts LiB and NF [panels b) and d)]. The geometric center of the molecules is located at $(x, z) = (0, 0)$. For the heteronuclear molecules, B and N are located at positive values of the z coordinate as indicated on the right-hand side of the figure. The orbital symmetries in panels a), b), c) and d) are $2\sigma_u$, 4σ, $1\pi_g$ and 2π, respectively, and the bond lengths are $R^{(\mathrm{Be_2})} = 4.642$ a.u., $R^{(\mathrm{LiB})} = 4.642$ a.u., $R^{(\mathrm{O_2})} = 2.280$ a.u., and $R^{(\mathrm{NF})} = 2.485$ a.u. For the heteronuclear molecules, the static dipole moments point towards the positive values of the z coordinate as shown by the arrows on the right-hand side of the figure. The static dipole moments computed considering only the charge cloud of the HOMO read $d_{LiB}^{(HOMO)} = 0.946132531$ a.u. and $d_{NF}^{(HOMO)} = 0.11647725$ a.u. for LiB and NF, respectively, while the total static dipole moments of both molecules are $d_{LiB} = 1.9895$ a.u. and $d_{NF} = 0.0407$ a.u.

the z-axis. The position-space wavefunctions of Be_2 and LiB are of σ type with Be_2 having ungerade symmetry, σ_u, and a nodal plane along the x-axis at $z = 0$. For LiB, there is a bias towards the Boron atom. One can also clearly see the contribution of the p type atomic orbital which is introduced by the Boron atom. This gives rise to a nodal structure of conical type, whose apex is displaced from $z = 0$ towards positive values of the z coordinate. The position-space wavefunctions of O_2 and NF are of π type with O_2 having gerade symmetry, π_g, and a nodal plane along the x-axis at $z = 0$ and the z-axis at $x = 0$. NF shows a bias towards the Nitrogen atom, so that the nodal plane along $z = 0$ in Fig. 1.(c) was distorted into a curved surface (see Fig. 1.(d)). In contrast, the plane along the x axis is left unaffected. In summary, Figs. 1.(c) and (d) show that the distortions of the electron charge cloud along the internuclear axis removes any nodal planes perpendicular to it for heteronuclear molecules. This implies that the probability density at the geometric center of the molecule is no longer vanishing, and that high-harmonic generation is no longer completely suppressed when what was a nodal plane in the homononuclear case is parallel to the laser-field polarization. This is particularly true if one assumes that the active electron returns to the geometric center of the molecule, as implicit in Eq. (12).

We have found that both momentum-space wavefunctions, whose absolute values are presented in Fig. 2 are symmetric with respect to $(p_x, p_z) \rightarrow (-p_x, -p_z)$ in

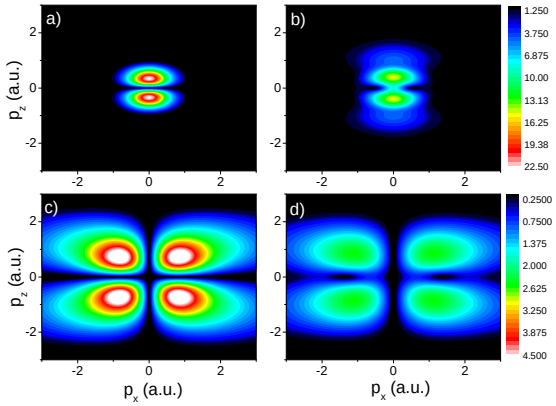

Figure 2. Absolute values of the highest occupied molecular orbitals in momentum space for the homonuclear molecule Be_2 and O_2 [panels a) and c), respectively] and their heteronuclear counterparts LiB and NF [panels b) and d), respectively].

comparison to their position-space counterparts. Despite that, the momentum-space wavefunctions for homonuclear and heteronuclear molecules exhibit different properties, especially if a real basis set is used in the construction of the position-space wavefunctions $\psi(\mathbf{r})$. They come from the properties of Fourier transforms and will determine whether a particular node will be blurred in the heteronuclear case. An even wavefunction in position space will lead to a real wavefunction in momentum space, as the Fourier transform of a real and even function should be real. For the same reason, if the position-space wavefunction is odd, the corresponding momentum-space wavefunction will be pure imaginary. Neither property will hold if the position-space wavefunction does not possess a well-defined symmetry. In this case, its momentum-space counterpart will be complex.

We will now have a closer look at the nodes in the momentum-space wavefunctions, whose absolute values are depicted in Fig. 2. For Be_2, the momentum-space wavefunction of the σ_u HOMO is pure imaginary, and exhibits a clear node along the p_x-axis (see Fig. 2.(a) for $|\psi(\mathbf{k})|$). This node is caused by the linear combination of atomic orbitals giving rise to the σ_u orbital. The above-mentioned node is lost in the absolute value of the HOMO momentum space wavefunction of LiB, as shown in Fig. 2.(b), even though a suppression along the p_x axis is still present. This feature is blurred by the real part of $\psi(\mathbf{k})$, which does not have this node, and is of comparable magnitude. We have also verified that this node is still present in $\mathrm{Im}[\psi(\mathbf{k})]$ (not shown). Hence, the loss of symmetry in position space is what leads to the loss of the clear nodal plane in momentum space.

In comparing O_2 and NF momentum space wavefunctions, one can see that the features are quite similar for one of the nodal planes. Specifically, the well defined nodal plane along the p_x-axis observed for O_2 has been slightly blurred for NF (see Figs. 2.(c) and (d), respectively). Note once more that an even and real position-space wavefunction, such as the HOMO in O_2, leads to a real momentum-space wavefunction.

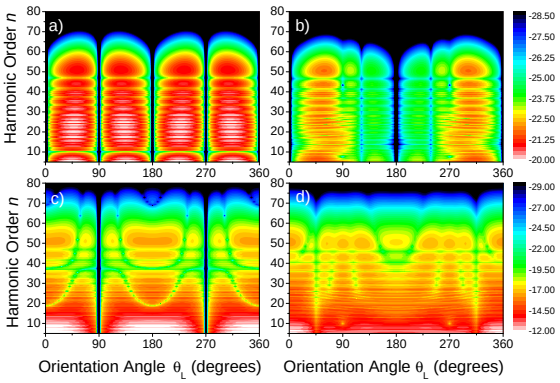

Figure 3. Harmonic spectra as a function of orientation angle for the molecule a) O_2 of ionization potential 0.2446 a.u., b) NF of ionization potential 0.2246 a.u., c) Be_2 of ionization potential 0.2390 a.u., and d) LiB of ionization potential 0.1942 a.u.. A linearly polarized laser field of frequency ω=0.057 a.u. and intensity $I = 4 \times 10^{14}\mathrm{W/cm}^2$ is used. The spectra have been computed using the length gauge and employing the dipole operator in the length form.

This is not the case for NF, and the non-vanishing imaginary part of the momentum space wavefunction gives rise to the blurring. Its imaginary part, however, is much smaller than its real part. This implies that the NF molecule is quite close to having gerade type symmetry, and therefore one would expect similar features in the position and momentum space wavefunctions as compared to those of O_2.

In contrast, the other nodal plane, along the z-axis, remains completely unaffected by the presence of the static dipole moment in NF. Indeed, this nodal plane is just as pronounced in both molecules, irrespective of being homonuclear or heteronuclear. Mathematically, this is because one can define two types of nodal structure in position space: one of which is due to the characteristic of the p-type atomic orbitals, and therefore disappear at $x = 0$, irrespective of the contraction coefficients and exponential coefficients, and the other of which is due to the linear combination of atomic orbitals. The latter results in a cancelation for a homonuclear molecule, and hence a nodal plane. This cancelation does not occur for a heteronuclear molecule. This argument can be mapped into the momentum space using Fourier transforms (see Eq. (5)). The nodal plane along the p_z-axis is of the first type, and is therefore present for both molecules, and the nodal plane along the p_x-axis is of the second type and not present for NF.

3.2. Harmonic Spectra

We now present the harmonic spectra computed in a linearly polarized monochromatic wave of frequency ω and amplitude ωA_0, for all molecules discussed previously. Unless otherwise stated, we will consider that the electron leaves and returns to the geometric center of the molecule, i.e., we will consider the action (3) and the saddle-point equations (11)-(13). These results are displayed in Fig. 3. It can be seen that all the spectra contain a series of cuts, i.e., a complete suppression of the yield for particular angles. Most notably in the case of O_2 these occur at orientation angles θ_L=0,90,180,270 and 360 degrees (see Fig. 3.(a))§. By observing the position space wavefunction in Fig. 1.(c) and the absolute value of the momentum space wavefunction in Fig. 2.(c) this can immediately be attributed to the nodal planes of the molecular wavefunction, which occur at these angles, and therefore prohibit ionization or recombination. The situation in the case of NF, however, is modified, as shown in Fig. 3.(b) for different orientation angles. The harmonic signal completely vanishes at orientation angles θ_L=0,180 and 360 degrees, because at these angles the nodal planes in the highest occupied molecular orbital occur due to the nature of the p-type atomic orbitals. However, due to the polar nature of these heteronuclear molecules, and a linear combination of atomic orbitals which no longer cancels out, the nodal planes at orientation angles θ_L=90 and 270 degrees are no longer present.

In fact, several differences with regard to the homonuclear case are observed. Firstly, the signal is no longer completely suppressed, but there is a distinct minimum which occurs at orientation angles (θ_L= 123 and 238 degrees). There is also a second minimum, but not a cut, beyond harmonic n=35, which occurs at the orientation angles θ_L=90 and 270 degrees, that is, where the nodes were in the homonuclear molecule. We attribute this to the remnants of the nodal plane in its heteronuclear counterpart.

Inspection of the position and momentum space wavefunction suggests that the polar nature of the heteronuclear molecules deforms the nodal plane such that, although there is no longer a node, there is a suppression which occurs at the angle to which the plane has been deformed. Hence, the probability density associated to the wavefunction is small, but nonvanishing. This leads to a minimum, but not a complete suppression in the spectrum. As the molecule is rotated the new minimum in the wavefunction is first experienced after θ_L=90 degrees but then occurs at the same angle before θ_L=270 degrees. Therefore the spectra has reflectional symmetry about an orientation angle of 180 degrees.

Note that, for O_2, the two-center interference maxima and minima predicted by Eq. (21) are located either beyond the cutoff or at the ionization threshold. Therefore, they do not occur in the parameter range of interest. This also holds for its heteronuclear counterpart.

Now observing the spectra for Be_2, displayed in Fig. 3.(c), one may identify nodes at θ_L=90 and 270 degrees, as one would expect by observing the position and momentum space wavefunctions. In the spectra of the heteronuclear counterpart LiB, presented in Fig. 3.(d), these nodes have been replaced by minima at θ_L=45 and 315

§ Note that orientation and alignment express different physical concepts. This is particularly relevant for heteronuclear molecules: whislt the permanent dipole moment of such molecules may be oriented parallel or antiparallel to the laser field polarization, the molecular axis may be aligned parallel to the laser field. This would mean that a parallel alignment alignment angle would be a coherent superposition of the parallel and antiparallel orientation. For homonuclear molecules, due to their inversion symmetry, in practice, parallel orientation means parallel alignment.

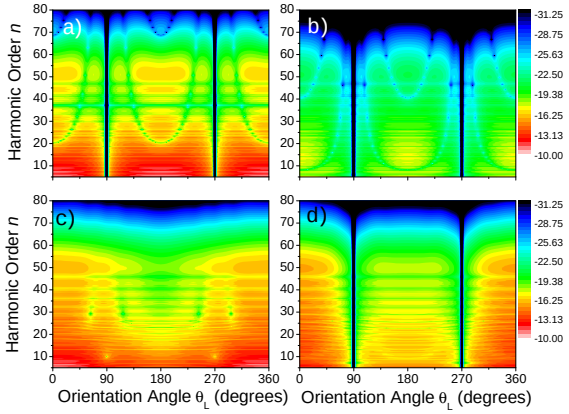

Figure 4. Harmonic spectra as a function of orientation angle for a) the s-type orbitals of the Be_2 HOMO, b) the p-type orbitals of the Be_2 HOMO, c) the s-type orbitals of the LiB HOMO, d) the p-type orbitals of the LiB HOMO, for the same parameters as in the previous figure.

degrees, for the same reasons as described above.

The spectra for Be_2 also exhibit two-center interference minima, corresponding to $\kappa = 0$, $\kappa = 1$ and $\kappa = 2$ in Eq. (20), whose energy position depends strongly on the orientation angle. These are shifted considerably in the heteronuclear counterpart LiB. This is because the Be_2 molecular wavefunction is constructed almost entirely of s-type atomic orbitals, whereas in the case of LiB the Boron atom introduces p-type atomic orbitals into the molecular wavefunction and hence changes the interference condition. Note that, with regard to Be_2, there is a blurring in the two-center patterns for LiB. This is expected according to the discussion in Sec. 2.3.

This is shown in more detail in Fig. 4, in which the individual contributions of the s and p states to the spectra of Be_2 and LiB are presented (upper and lower panels, respectively). For these individual contributions, there is also a considerably simpler interference condition for homonuclear molecules, which can be obtained from Eq. (20) by setting either C_+ or C_- equal to zero. Specifically the s-state and p-state contributions for an ungerade orbital exhibit minima at the harmonic frequencies

$$\Omega_s^{(u)} = E_0 + \frac{2\kappa^2\pi^2}{R^2\cos^2\theta_L} \tag{22}$$

and

$$\Omega_p^{(u)} = E_0 + \frac{(2\kappa+1)^2\pi^2}{2R^2\cos^2\theta_L}, \tag{23}$$

respectively, where κ is a integer. In Fig. 4.(a), we may identify the minima for $\kappa = 1$ and $\kappa = 2$ according to Eq. (22), while in Fig. 4.(b) the minima corresponding to $\kappa = 0$ and $\kappa = 1$ can be easily found. If the s p mixing is considered, the full expression (20) must be used.

The contributions from p-type orbitals to the harmonic spectrum of Be_2 are orders of magnitude smaller than the contribution of p-type orbitals in LiB. Therefore the overall spectrum of Be_2 is dominated mostly by the s-type atomic orbitals. In contrast, in LiB, both types of orbitals lead to comparable contributions to the spectra, and

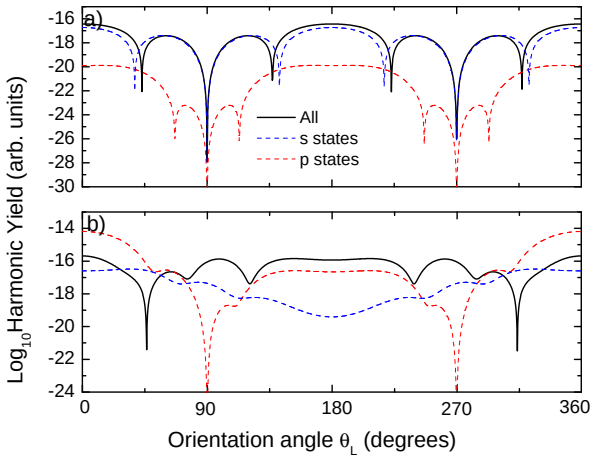

Figure 5. Contributions of the s, p and all atomic orbitals to the yield of the 25^{th} harmonic of a) Be_2 and b) LiB as functions of the orientation angle θ_L. All parameters are the same as in the previous figure.

the s p mixing will influence the energy position of the overall LCAO patterns. Apart from that, the ionization potentials and internuclear separation of both molecules are slightly different. This will influence the interference condition (20) further.

The effects of s p mixing are also displayed in Fig. 5.(a) and Fig. 5.(b) for a fixed mid-plateau harmonic. The figure clearly shows that where one observes that, for Be_2, the s-type orbitals dominate and the main effect of the p-type orbitals is to introduce a small shift in the interference minima. On the other hand, for LiB, the overall maxima and minima are considerably altered by s p mixing. In the figure, one can also see that the nodal planes occurring at orientation angles θ_L=90 and 270 degrees in Be_2, are shifted by the contribution of the s-type orbitals in LiB.

In the results discussed so far, we have assumed that the electron left and returned to the geometric center of the molecule. In other words, all the molecular structure has been incorporated into the prefactor. However, a legitimate question would be how the present results would change if instead, the action contained the molecular structure. In the latter case, there will be four different geometric paths along which the electron may return and the so called " exchange harmonics", in which one electron leaves from one ion and recombines with the other, are expected to play a role.

In Fig. 6, we exhibit the intensity of a plateau harmonic for O_2 and NF computed with both methodologies. As previously discussed, both molecules exhibit two types of nodal structures, which are either determined by either the LCAO or the properties of the atomic wavefunctions only.

For O_2 (Fig. 6.(a)), we find that the yield computed using both methods is very similar, with a strong suppression for both types of nodal planes. In fact, the only differences encountered are small changes in the overall yield. In contrast, for NF (Fig. 6.(b)), the suppression due to the nodal structure related to the LCAO is considerably reduced. This can be understood as follows. In the modified-prefactor

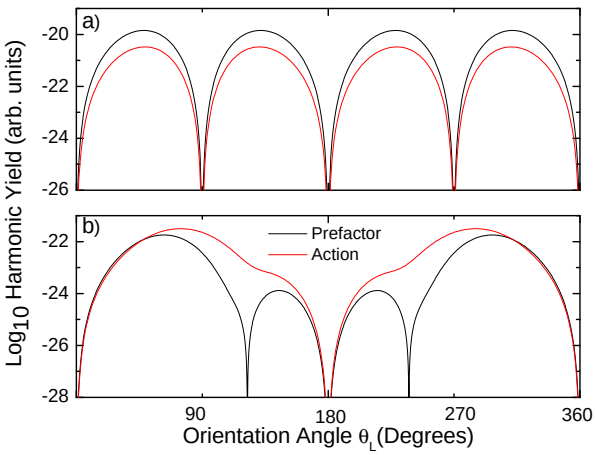

Figure 6. The harmonic yield of a) O_2 and b) NF for the 25^{th} harmonic vs the orientation angle, computed using either a modified prefactor and single-atom saddle-point equations, or a modified action (black and red lines, respectively). All parameters are the same as in the previous figure.

computation, the main emphasis is on the shape of the molecular wavefunction. For the heteronuclear case, this wavefunction has been deformed such that it is no longer vanishing at the geometric center of the molecule. Hence, the nodal structure is still present, even though it is observed for a different angle. However, the electron is always returning to the geometric center of the molecule.

In contrast, in the modified-action picture, one may view the suppression at the LCAO nodes as the quantum interference due to recombination at spatially separated centers. Hence, the molecule behaves as the microscopic counterpart of a double slit experiment. If the centers in the molecule are identical, then the electron orbits will interfere as if they were leaving from identical "slits". Thus, sharp two-center interference patterns are expected. If, however, the molecule is heteronuclear, this implies that one of such "slits" is larger than the other, i.e., that the contributions from one center of the molecule will dominate. Hence, the nodes caused by the quantum interference of different geometrical paths will be less distinct.

4. Conclusions

In this work, we investigated the dependence of the high-order harmonic spectra on the orientation angle between the diatomic molecules and the laser-field polarization, for isoelectronic pairs consisting of a homonuclear and a heteronuclear molecule. We employed a single active electron approximation, using the HOMO as the active orbital, within the strong-field approximation.

Our studies lead us to conclude that there are two types of nodal structures in the bound-state orbitals of molecules, which will lead to a strong suppression in the harmonic yield when such structures are parallel to the laser–field polarization. The

first type is caused by the nodes in the atomic orbitals at *each* ion, and is present at the same location for homonuclear molecules and their heteronuclear counterparts. The second type is due to the sum or subtraction of atomic orbitals at *different* centers within the linear combination of atomic orbital (LCAO) approximation. Both types of minima are present for homonuclear molecules. For their heteronuclear counterparts, however, the asymmetry of the molecule eliminates the latter nodes. This implies that the imprints of the first type of nodes in the harmonic spectra are common to isoelectronic homonuclear and heteronuclear molecules, and could in principle be observed in both cases.

In general, the asymmetry also leads to some blurring in the interference patterns determined by the LCAO at different centers. Furthermore, depending on the molecule, s p mixing will be different. This will lead to shifts in the energy positions of the two-center patterns. On a more technical level, we have also been able to map the symmetry or asymmetry of the molecular orbitals in position space to properties of their momentum-space counterparts. Apart from that, if one considers that the electron travels different paths in the molecule, returning to the right or left ions instead of to its geometric center, additional blurring will be observed for the two-center nodes in the heteronuclear case.

The above-stated findings show that nodal structures in a heteronuclear molecule can be related to those in an isoelectronic homonuclear molecule. Hence, in principle, the latter can be used as a reference point in order to understand the behavior of the former, by using high-order harmonic generation. The shifts in the nodal planes present for homonuclear molecules due to the distortions in the wavefunctions, or the absence thereof, can be mapped into features in the high-harmonic spectra. This is a very good example of how symmetry breaking in a molecule reflects itself in the harmonic spectra, may shed some light in the imaging of heteronuclear molecules. Another example of this are the even harmonics, which are present in oriented heteronuclear molecules (for a recent example see [12]).

Finally, we would like to comment on the fact that, throughout this work, the Stark shifts in the ionization potentials of the molecules have been neglected in the strong-field approximation. The first-order shifts lead to binding energies which depend on the alignment angle. In fact, if the static dipole moment is oriented parallel or antiparallel to the laser-field polarization, the bound-state energies will decrease, or increase, respectively. This would imply a shift in the cutoff towards higher energies in the antiparallel case. The second-order shifts are much smaller and do not depend on the alignment angle. For homonuclear molecules, the first-order Stark shift is vanishing, so that orientation effects can be neglected. For heteronuclear molecules such as NF, for which the static dipole moment is small, the Stark shift is expected to be negligible. For LiB, however, the static dipole moment is much larger. Hence, further distortions in the spectra due to the above-mentioned effect are expected ‖.

Acknowledgments

We thank H. J. J. van Dam, P. J. Durham, P. Sherwood and J. Tennyson for very useful discussions. This work was supported by the UK Engineering and Physical Sciences Research Council (EPSRC), and by the Daresbury Laboratory.

‖ For orientation angles $0 < \theta_L < \pi/2$ and $3\pi/2 < \theta_L < 2\pi$ the Stark shift will lower the potential barrier and cause a decrease in the high-harmonic cutoff, while for $\pi/2 < \theta_L < 3\pi/2$ the opposite will occur and the cutoff will increase. For perpendicular orientations, there is no Stark shift.

[1] McPherson A, Gibson G, Jara H, Johann U, Luk T S, McIntyre I A, Boyer K, and Rhodes C K 1987 *J. Opt. Soc. Am. B* **4**, 595.

[2] Lewenstein M, Balcou Ph, Ivanov M Yu, L'Huillier A and Corkum P B 1994 *Phys. Rev. A* **49**, 2117.

[3] Corkum P B 1993 *Phys. Rev. Lett.* **71**, 1994.

[4] Kanai T, Minemoto S and Sakai H 2005 *Nature* **435**, 470.

[5] Itatani J, Levesque J, Zeidler D, Niikura H, Pépin H, Kieffer J C, Corkum P B and Villeneuve D M 2004 *Nature* **432**, 867.

[6] Smirnova O, Mairesse Y, Patchkovskii S, Dudovich N, Villeneuve D, Corkum P B, Ivanov M Y 2009 *Nature* **460**, 972.

[7] Lein M, Hay N, Velotta R, Marangos J P, and Knight P L 2002 *Phys. Rev. Lett.* **88**, 183903; 2002 *Phys. Rev. A* **66**, 023805; Spanner M, Smirnova O, Corkum P B and Ivanov M Y 2004 *J. Phys. B* **37**, L243.

[8] Milošević D B 2006 *Phys. Rev. A* **74**, 063404; Busuladžić M, Gazibegović-Busuladžić A, Milošević D B, and Becker W 2008 *Phys. Rev. Lett.* **100**, 203003; 2008 *Phys. Rev. A* **78**, 033412.

[9] Madsen C B and Madsen L B, 2006 *Phys. Rev. A* **74**, 023403; Madsen C B, Mouritzen A S, Kjeldsen T K, and Madsen L B, 2007 *Phys. Rev. A* **76**, 035401.

[10] Chu X and Chu S I, 2001 *Phys. Rev. A* **64**, 063404; Telnov D A and Chu S- I 2009, *Phys. Rev. A* **80**, 043412; Chu X and Chu S I; 2004 *Phys. Rev. A* **70**, 061402; Son S -K and Chu S I 2009 *Phys. Rev. A* **80**, 011403.

[11] Stapelfeldt H and Seideman T 2003 *Rev. Mod. Phys.* 75 543; De S et al 2009 *Phys. Rev. Lett.* 103 153002; Holmegaard L, Nielsen J H, Nevo I, Stapelfeldt H, Filsinger F, Küpper J and Meijer G 2009 Phys. Rev. Lett. 102 023001; Holmegaard L, Hansen J L, Kalhøj L, Kragh S L, Stapelfeldt H, Filsinger F, Küpper J, Meijer G, Dimitrovski D, Abu-samha M, Martiny C P J, and Madsen L B 2010 *Nature Phys.* **6**, 428

[12] Etches A and Madsen L B 2010 *J. Phys. B* **43**, 155602.

[13] Dimitrovski D., Martiny C P J and Madsen L B 2010 *Phys. Rev. A* **82**, 053404

[14] GAMESS-UK is a package of ab initio programs. See: "http://www.cfs.dl.ac.uk/gamess-uk/index.shtml", Guest M F, Bush I J, van Dam H J J, Sherwood P, Thomas J H, van Lenthe J H, Havenith R W A, Kendrick J 2005 *Mol. Phys.* **103**, 719.

[15] Figueira de Morisson Faria C and Augstein B B 2010 *Phys. Rev. A* **81**, 043409.

[16] Patchkovskii S, Zhao Z, Brabec T and Villeneuve D M 2006 *Phys. Rev. Lett.* **97**, 123003; Patchkovskii S, Zhao Z, Brabec T, and Villeneuve D M, 2007 *J. Chem. Phys.* **126**, 114306; Smirnova O, Patchkovskii S, Mairesse Y, Dudovich N, Villeneuve D, Corkum P B, and Ivanov M Yu 2009 *Phys. Rev. Lett.* **102**, 063601.

[17] Smirnova O, Spanner M and Ivanov M, 2007 *J. Mod. Opt.* **54**, 1019.

[18] Figueira de Morisson Faria C 2007 *Phys. Rev. A* **76**, 043407

[19] Figueira de Morisson Faria C, Schomerus H and Becker W 2002 *Phys. Rev. A* **66**, 043413.

[20] Augstein B B and Figueira de Morisson Faria C, arXiv: 1007.2135 [atom.ph]

[21] Odžak S and Milošević D B 2009 *Phys. Rev. A* **79**, 023414; 2009 *J. Phys. B* **42**, 071001.

[22] Kopold R., Becker W. and Kleber M. 1998 *Phys. Rev. A* **58**, 4022.

[23] Chirilă C. C. and Lein M. 2006 *Phys. Rev. A* **73**, 023410.

[24] Etches, A., Madsen, C. B., and Madsen, L. B. 2010 *Phys. Rev. A* 81, 013409